

# Flow noise in sonar applications

Christian Henke<sup>1</sup>

<sup>1</sup> *Atlas Elektronik GmbH, 28309 Bremen, Germany, Email: christian.henke@atlas-elektronik.com*

April 11, 2016

## Abstract

In this paper we present an investigation of flow noise in sonar applications. Based on a careful identification of the dominant coupling effects, the acoustic noise at the sensor position resulting from the turbulent wall pressure fluctuations is modelled with a system of hydrodynamic, bending and acoustic waves. We describe an analytical solution of the problem which is based on a coupled eigenfunction expansion method. Finally, it is demonstrated that the analytical solution describes the flow noise generation and propagation mechanisms of the considered sea trials.

## 1 Introduction

Most vehicle mounted hydrophones used in passive sonar sensors are mounted inside stiff sonar windows in order to protect the sensors and to reduce the hydrodynamical drag/vibrations of the sensors. On the one hand, when the vessel is in motion, the structure is excited by turbulent flow, and on the other hand, the generated turbulence causes additional noise. Thus, the acoustic waves of these contributions propagate to the position of the hydrophone and disturb the incoming signal. The aim of the paper is an investigation of flow noise generation and transport mechanisms w.r.t. different materials and geometries. The knowledge of these mechanisms could be used to maximize the signal to noise ratio. The mathematical modeling and a combined numerical/analytical solution of passive sonar acoustics will be validated against experiments. In order to consider real life underwater scenarios, the experiments involve sea trials with a test towed body, which realizes a typical broadband sonar environment (cf. [AK16]). On the starboard side, the hull of the test towed body includes a linear elastic plate, which is in front of the measurement system. This system consists of a line array having equally spaced hydrophones inside a water-filled measurement box, which is designed to protect the sensors from background noise. Furthermore, the box is mounted in such a way that it is decoupled from the body frame. In this way noise from the environment conditions could be minimised. The flow noise generation and transport mechanisms of the sonar configuration under consideration are investigated by a wave-number-frequency analysis.

The outline of the paper is as follows. In section 2 we identify the dominant flow noise sources by a dimensional analysis of the Williams and Hawkins equation (cf. [WH69, p. 331], [Ho98, p. 114]). In section 3 we describe these noise sources and the underlying coupling effects by a set of partial differential equation and boundary conditions. As a first test of the modeling approach, the coupled problem is solved by a Finite Element Method and compared with the sea trial results. Then, in section 4, we give the analytical solutions of the problems with the help of an eigenfunction expansion method.

## 2 Dominant flow noise sources

From the point of view of dimensional analysis, which considers the relationships between the hydrodynamical and acoustic quantities, it is impossible to attack the problem at once. Therefore, we use a non-empirical tailoring which is tractable with state of the art analytical and numerical methods and considers the conditions of the towed body. In order to meet this demand, this section is devoted to the investigation of the dominant flow noise sources.

The physical mechanisms of flow noise generation and propagation in air and water is governed by the Navier-Stokes equation. Because of the same underlying equation for the density  $\rho$ ,

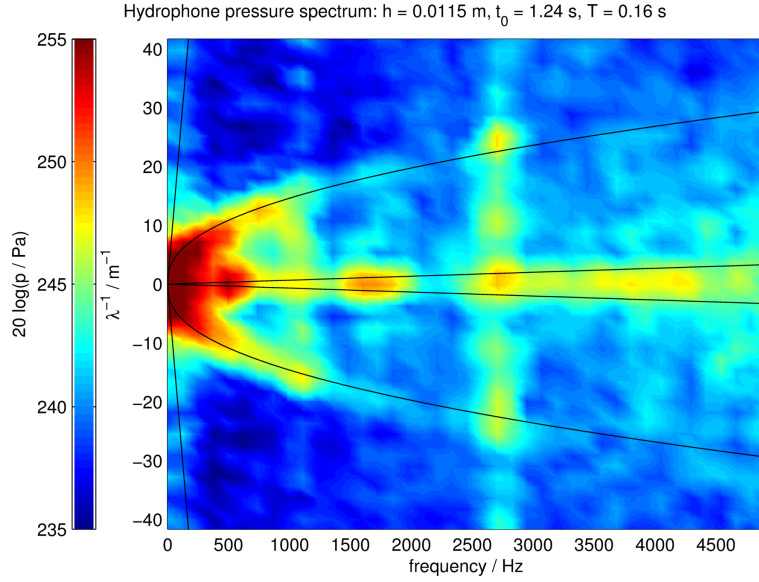


**Figure 1:** Sound Pressure Level (Sea trial experiment: [AK16]): wave-number-frequency plot for towing speed  $u = 4\text{kn}$  and a hydrophone distance of  $0.01\text{m}$ . The straight lines show the relations  $\lambda^{-1} = u^{-1}f$  and  $\lambda^{-1} = c^{-1}f$ , where the curved line plots the dispersion relation which is investigated in the following sections. The dominant noise at  $2700\text{ Hz}$  is caused by the environment conditions.

the velocity  $u$  and the pressure  $p$ , it seems surprising that the fields of aeroacoustics and hydroacoustics have developed relatively independently of each other. However, if we realise that the different compressibility of both media are responsible for different dominant flow noise sources, this development becomes easy to understand and help us to choose the correct mathematical modelling. To investigate the flow noise sources we consider an isentropic flow with  $p' = c^2 \rho'$ ,  $p' = p - \bar{p}$ ,  $\rho' = \rho - \bar{\rho}$ . Here and in what follows,  $\bar{\cdot}$  denotes the space-time average. For a given domain  $V$  with surfaces  $S$ , we introduce Lagrangian coordinates  $\eta(y, \tau)$  and the notations

$$r = \|x - y(\eta, \tau)\|, \quad y(\eta, \tau) = \eta + \int^\tau v(\eta, \tau') d\tau', \quad (1)$$

$$M_r(\eta, \tau) = \frac{x - y(\eta, \tau)}{r} \cdot \frac{v(\eta, \tau)}{c},$$

where  $v$  denotes the velocity related to the fixed  $y$ -frame. With respect to the isentropy assumption, the equation of Williams and Hawkings [WH69, p. 331], [Ho98, p. 114] provides an equivalent formulation of the compressible Navier-Stokes equation such that Lighthill's wave equation is extended with the sound sources caused by body vibrations

$$p'(t, x) = \frac{1}{4\pi} \nabla \cdot \nabla \cdot \int_V \left[ \frac{(\rho u \otimes u - \tau) J}{r|1 - M_r|} \right]_{\text{ret}} d\eta$$

$$- \frac{1}{4\pi} \nabla \cdot \int_S \left[ \frac{(p' I - \tau) n A}{r|1 - M_r|} \right]_{\text{ret}} dS(\eta)$$

$$+ \frac{1}{4\pi} \partial_t \int_S \left[ \frac{\bar{\rho} u \cdot n A}{r|1 - M_r|} \right]_{\text{ret}} dS(\eta), \quad (2)$$

where  $\tau$  is the viscous stress tensor and  $J$  and  $A$  denotes the volume and surface Jacobian. Here, the bracket  $[\cdot]_{\text{ret}}$  requires the evaluation at the implicitly given retarded time  $\tau = t - r(\tau)/c$ . In order to identify the dominant terms on the right hand side, we write equation (2) in a dimensionless form. For simplicity of notation, we replace

$$\begin{aligned} t &\rightarrow \frac{tu_R}{x_R}, & x &\rightarrow \frac{x}{x_R}, & y &\rightarrow \frac{y}{x_R}, \\ p &\rightarrow \frac{\bar{p}}{\rho_R c_R^2}, & u &\rightarrow \frac{u}{u_R}, & v &\rightarrow \frac{v}{u_R}, \\ \rho &\rightarrow \frac{\rho}{\rho_R}, & c &\rightarrow \frac{c}{c_R}, & \mu &\rightarrow \frac{\mu}{\mu_R}, \end{aligned}$$

where variables with index  $R$  denote some reference variables. Consequently, it follows that

$$\begin{aligned} p'(t, x) = & \frac{1}{4\pi} \nabla \cdot \nabla \cdot \int_V \left[ \frac{(M^2 \rho u \otimes u - \frac{M^2}{\text{Re}} \tau) J}{r |1 - M M_r|} \right]_{\text{ret}} d\eta \\ & - \frac{1}{4\pi} \nabla \cdot \int_S \left[ \frac{(p' I - \frac{M^2}{\text{Re}} \tau) n A}{r |1 - M M_r|} \right]_{\text{ret}} dS(\eta) \\ & + \frac{1}{4\pi} \partial_t \int_S \left[ \frac{M^2 \bar{\rho} u \cdot n A}{r |1 - M M_r|} \right]_{\text{ret}} dS(\eta), \end{aligned}$$

where  $M = \frac{u_R}{c_R}$  and  $\text{Re} = \frac{\rho_R u_R x_R}{\mu_R}$  are the global Mach and Reynolds number. Obviously, the second term on the right hand side and therefore the structural vibrations are the dominant sound sources for practical hydrodynamic flows ( $M^2 \ll 1$ ). In other words, the following tailoring approach could neglect the volume based turbulent flow noise and should take into account the plate vibrations.

### 3 Tailoring approach

In order to describe the interaction of the flexible plate with the turbulent flow outside and the acoustic waves inside the measurement box, it is assumed that there is no feedback of the plate vibrations on the turbulent flow (single side coupling). Namely, the hydrodynamic pressure is added as a source term in the two side coupling of bending and acoustic waves. The validity of this hybrid approach is investigated by the evaluation of the acoustic pressure in the frequency/wave number domain. This way, we can check if the source term interpretation of the hydrodynamic flow leads to valid transport mechanisms of the coupled waves.

In this approach, we have to start with a broadband hydrodynamical field in a computational domain over the sonar window. To meet this demand, the incompressible Navier-Stokes equations are solved by a Large Eddy Simulation (LES), where the larger scales are resolved and the effects on the smaller scales are considered by a subgrid-scale model. Moreover, the LES simulation requires turbulent inflow data, which is obtained by an auxiliary simulation with obstacles mounted at the wall [WHea07, Section 5.2.2.].

Finally, the coupling of the plate vibrations with the acoustic field has to be solved. Here, it is assumed that the vibrations of a plate with thickness  $h$  and displacements  $w$  satisfy the following condition

$$w \ll h \ll \text{wavelength of the bending waves.} \quad (3)$$

Then the displacement  $w$  takes place only in the perpendicular direction. Therefore, the acoustic interaction appears only in the same direction. Consequently, the tangential domain boundaries and the associated acoustic boundary conditions in the measurement box are of minor importance and could be considered as a sound hard wall on a rectangular wall. In order to represent the material properties of the measurement box, the wall on the back side is equipped with an impedance boundary condition.

Next, the mathematical problem and a connected numerical simulation of the coupled acoustic and bending wave problem are presented.

We start by introducing the modelling domain, which was already mentioned in a loose way in the introduction. Let the measurement box be a rectangular domain  $\Omega = (-l_1/2, l_1/2) \times (-l_2/2, l_2/2) \times (-l_3/2, l_3/2)$  with the side lengths  $l_1, l_2, l_3$ . The plate with uniform thickness  $h$  is located at  $\Gamma = \{x \in \Omega : x_3 = 0\}$ . Moreover, the hydrophones are mounted on the line  $H = \{x \in \Omega : x_2 = 0, x_3 = l\}$ , where  $l < 0$  is a given parameter.

Taking the assumption (3), we can reduce the complexity of linearised elasticity by an application of the bending wave equation

$$m \partial_t^2 w + B \Delta \Delta w = -(p^+ - p^-), \quad \text{on } [0, T] \times \Gamma, \quad (4)$$

where  $m = \rho_p h$ ,

$$B = \frac{E h^3}{12(1 - \nu^2)}, \quad (5)$$

is the bending stiffness and  $p^+, p^-$  are the pressures above and below the plate [Ho98, p. 17]. Namely,  $p^+$  corresponds to the hydrodynamic pressure and  $p^-$  to the acoustic pressure, respectively. Moreover,  $p^-$  satisfies the usual wave equation

$$-\frac{1}{c^2}\partial_t^2 p^- + \Delta p^- = 0, \quad \text{on } [0, T] \times \{x \in \Omega : x_3 < 0\}, \quad (6)$$

which interacts additionally on  $[0, T] \times \Gamma$  by

$$\partial_t^2 w = -\frac{1}{\rho_w} \partial_{x_3} p^-. \quad (7)$$

Here,  $c$  and  $\rho_w$  denotes the speed of sound and the density of water. It remains to specify the boundary conditions for the plate and the measurement box. The wall displacement satisfies the plate boundary conditions

$$\begin{aligned} w(t, -l_1/2, x_2) &= w(t, l_1/2, x_2) = w(t, x_1, -l_2/2) = w(t, x_1, l_2/2) = 0, \\ \partial_{x_1}^2 w(t, -l_1/2, x_2) &= \partial_{x_1}^2 w(t, l_1/2, x_2) = 0 \text{ (simply supported)}, \\ \partial_{x_2}^2 w(t, x_1, -l_2/2) &= \partial_{x_2}^2 w(t, x_1, l_2/2) = 0 \text{ (simply supported)}, \end{aligned} \quad (8)$$

and the pressure conditions for the side and rear walls

$$\begin{aligned} \partial_{x_1} p(t, -l_1/2, x_2, x_3) &= \partial_{x_1} p(t, l_1/2, x_2, x_3) = 0 \text{ (sound hard wall)}, \\ \partial_{x_2} p(t, x_1, -l_2/2, x_3) &= \partial_{x_2} p(t, x_1, l_2/2, x_3) = 0 \text{ (sound hard wall)}, \\ \rho_w^{-1} \partial_{x_3} p(t, x_1, x_2, -l_3/2) &= -z^{-1} \partial_t p(t, x_1, x_2, -l_3/2) = 0 \text{ (impedance)}, \end{aligned} \quad (9)$$

where  $z$  denotes the acoustic impedance.

At the end of this section, we present numerical results of the above problem, which are obtained by a usual Finite Element Method with second order polynomial shape functions. For the time discretisation the Generalised- $\alpha$  method with the damping parameter  $\rho_\infty = 0.02$  is used (cf. [CH93],[JWH00]). Notice that for higher values of  $\rho_\infty$  (lower damping) no convergence is reached. The underlying mesh is quadrilateral with a maximal mesh size of 0.005m.

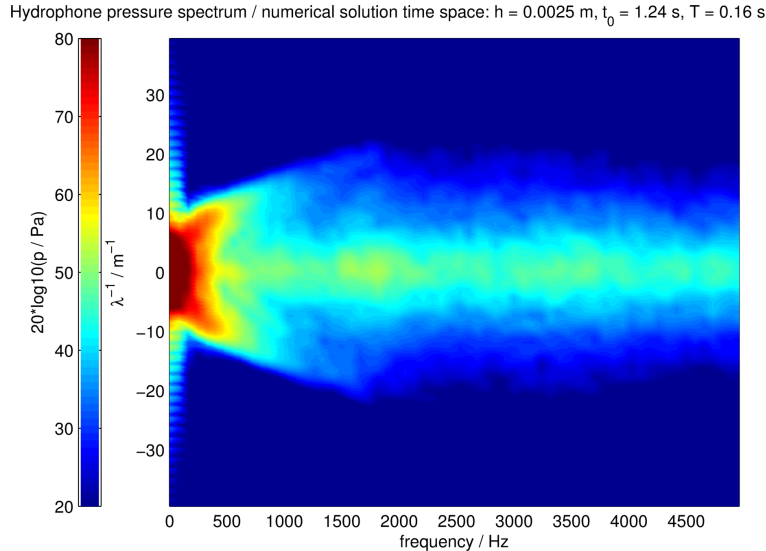


**Figure 2:** Sound Pressure Level (FEM, time domain): wave-number-frequency plot for towing speed  $u = 4\text{kn}$  and a hydrophone distance of 0.01m.

The numerical result from Figure 2 indicates that our tailoring approach captures the relevant noise generation and propagation mechanisms. Especially, the envelope and the damping at higher frequencies agree very well with the sea trial results.

In order to investigate the influence of the time discretisation scheme, we discretise the problem in the frequency domain and use a fourier decomposition of the LES results as the hydrodynamic source term.

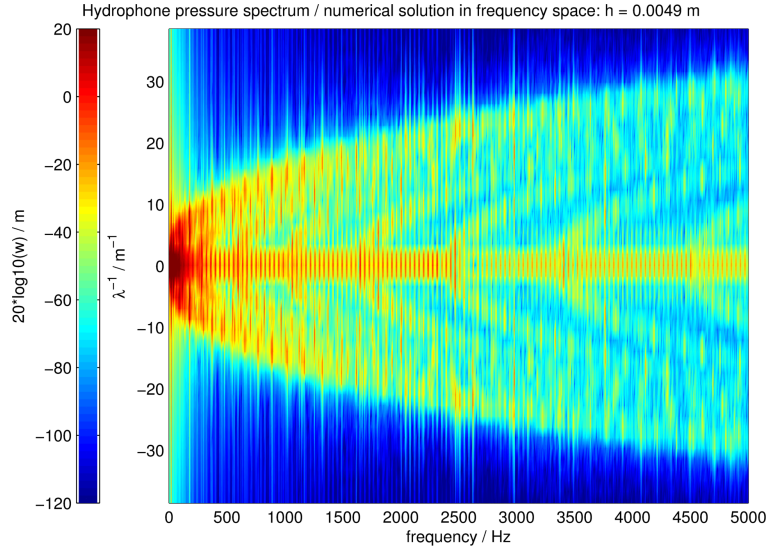


**Figure 3:** Sound Pressure Level (FEM, frequency domain): wave-number-frequency plot for towing speed  $u = 4\text{kn}$  and a hydrophone distance of  $0.01\text{m}$ .

Now, we can see the undamped noise propagation mechanisms in Figure 3. The large differences between the damped and undamped noise propagation indicates the great importance of damping phenomena in the modelling process. Surprisingly, the damping effects of the time discretisation agrees very well with the damping of the real configuration.

## 4 Analytic solution of the acoustic/bending wave problem

In this section, we demonstrate the analytical solution of the two side coupled problem. Thanks to the rectangular domain, the displacement and the acoustic pressure can be written as a linear combination of product basis functions

$$\begin{aligned} w(t, x_1, x_2) &= \Re \left\{ \sum_{n_0, n_1, n_2 \in \mathbb{Z}} w_n w_{n_0}(t) w_{n_1}(x_1) w_{n_2}(x_2) \right\} \quad \text{on } [0, T] \times \Gamma, \\ p^-(t, x_1, x_2, x_3) &= \Re \left\{ \sum_{n_0, n_1, n_2, n_3 \in \mathbb{Z}} p_n p_{n_0}(t) p_{n_1}(x_1) p_{n_2}(x_2) p_{n_3}(x_3) \right\} \quad \text{on } [0, T] \times \Omega. \end{aligned} \quad (10)$$

In order to prepare the frequency/wave-number analysis of the hydrophone signals, we assume that  $w_{n_i}, p_{n_i}$ ,  $i = 0, \dots, d$ ,  $n_0 = -f$ , are periodic functions and introduce the notations

$$\langle v, w \rangle = \int_{-\frac{T}{2}}^{\frac{T}{2}} \int_{-\frac{l_1}{2}}^{\frac{l_1}{2}} \int_{-\frac{l_2}{2}}^{\frac{l_2}{2}} v(t, x_1, x_2) \overline{w(t, x_1, x_2)} dt dx_1 dx_2, \quad \|v\| = \sqrt{\langle v, v \rangle},$$

where  $v, w : [0, T] \times \Gamma \rightarrow \mathbb{R}$  are also periodic functions. Now, we can write the Fourier series representation as follows

$$\begin{aligned} v(t, x_1, x_2) &= \sum_{n \in \mathbb{Z}^3} \frac{\langle v, \Psi_n \rangle}{\|\Psi_n\|^2} \Psi_n, \\ \Psi_n(t, x_1, x_2) &= \exp \left( i2\pi \left( -\frac{ft}{T} + \frac{n_1 x_1}{l_1} + \frac{n_2 x_2}{l_2} \right) \right). \end{aligned} \quad (11)$$

Then, using integration by parts, it is straightforward to verify for  $v : [0, T] \times \Gamma$  the identities

$$\begin{aligned}\langle \partial_t v, \Psi_n \rangle &= ik_0 \langle v, \Psi_n \rangle, \quad k_0 = -\frac{2\pi f}{T} = -\omega, \\ \langle \partial_{x_j}^\alpha v, \Psi_n \rangle &= (ik_j)^\alpha \langle v, \Psi_n \rangle, \quad k_j = \frac{2\pi n_j}{l_j}, \quad j = 1, 2, \quad \alpha \in \mathbb{N}, \\ \langle \Delta v, \Psi_n \rangle &= -k^2 \langle v, \Psi_n \rangle, \quad k^2 = k_1^2 + k_2^2.\end{aligned}\tag{12}$$

#### 4.1 Eigenfunctions of the acoustic and bending waves

Using the product basis, one can construct eigenfunctions which satisfy the correct boundary conditions, by one-dimensional arguments.

Substituting an approach of the form

$$\begin{aligned}w_{n_0}(t) &= \exp(-i\omega t), \\ w_{n_j}(x_j) &= \sin(\tilde{k}_j x_j), \quad \tilde{k}_j = \frac{n_j \pi}{l_j}, \quad j = 1, 2,\end{aligned}\tag{13}$$

in (10), the displacement  $w$  solves the homogeneous form of (4) if

$$\omega = \pm \left( \frac{B}{m} \right)^{1/2} \tilde{k}^2, \quad \tilde{k}^2 = \tilde{k}_1^2 + \tilde{k}_2^2,\tag{14}$$

is fulfilled. Moreover, we find the acoustic eigenfunctions by separation of variables. Namely, (6) is satisfied by (10) if we claim

$$\begin{aligned}p_{n_0}(t) &= \exp(-i\omega t), \\ p''_{n_j}(x_j) + k_{n_j}^2 p_{n_j}(x_j) &= 0, \quad j = 1, 2, 3, \\ \frac{\omega^2}{c^2} &= k_1^2 + k_2^2 + k_3^2.\end{aligned}\tag{15}$$

The boundary conditions (9) are fulfilled if we implement

$$\begin{aligned}p'_{n_j}(-l_j/2) &= p'_{n_j}(l_j/2) = 0, \quad j = 1, 2, \\ \frac{1}{\rho_w} p'_{n_3}(-l_3/2) &= \frac{i\omega}{z} p_{n_3}(-l_3/2).\end{aligned}\tag{16}$$

Therefore, we obtain

$$p_{n_j}(x_j) = \cos(k_j x_j), \quad j = 1, 2,\tag{17}$$

and with a short calculation based on a sum of an incident and a reflected wave, the impedance boundary condition is satisfied by

$$p_{n_3}(x_3) = \alpha_n \left[ \exp(ik_3 x_3) + \frac{k_3 z - \omega \rho_w}{k_3 z + \omega \rho_w} \exp(-ik_3 l_3) \exp(-ik_3 x_3) \right], \quad \alpha_n \in \mathbb{C}.\tag{18}$$

#### 4.2 Solution of the coupled problem

Inserting the eigenfunctions into (10) and using (15), the summation w.r.t.  $n_3$  reduces to one term concerning  $k_3 = \sqrt{(\omega^2/c^2 - k_1^2 + k_2^2)}$ . Thus we can write

$$\begin{aligned}w(t, x_1, x_2) &= \Re \left\{ \sum_{n_0, n_1, n_2 \in \mathbb{Z}} w_n \exp(-i\omega t) \sin(\tilde{k}_1 x_1) \sin(\tilde{k}_2 x_2) \right\}, \\ p^-(t, x_1, x_2, x_3) &= \Re \left\{ \sum_{n_0, n_1, n_2 \in \mathbb{Z}} p_n^- \exp(-i\omega t) \cos(k_1 x_1) \cos(k_2 x_2) \times \right. \\ &\quad \left. \times \left( \exp(ik_3 x_3) + \frac{k_3 z - \omega \rho_w}{k_3 z + \omega \rho_w} \exp(-ik_3 l_3) \exp(-ik_3 x_3) \right) \right\}.\end{aligned}\tag{19}$$

Notice that the coefficient  $\alpha_n$  from (18) is accounted by  $p_n^-$ . Now, in order to determine the coefficients  $w_n$  and  $p_n^-$ , it remains to consider the two side coupling by (4) and (7). To do so, we define

$$\begin{aligned}\Phi_n(t, x_1, x_2) &= \exp(-i\omega t) \sin(\tilde{k}_1 x_1) \sin(\tilde{k}_2 x_2), \\ \Theta_n(t, x_1, x_2) &= \exp(-i\omega t) \cos(k_1 x_1) \cos(k_2 x_2), \\ \Theta_{n_3}(x_3) &= \exp(ik_3 x_3) + \frac{k_3 z - \omega \rho_w}{k_3 z + \omega \rho_w} \exp(-ik_3 l_3) \exp(-ik_3 x_3),\end{aligned}\tag{20}$$

and write the two side coupling for every  $m \in \mathbb{Z}^3$  in the following manner:

$$\begin{aligned}m \langle \partial_t^2 w, \Psi_m \rangle + B \langle \Delta \Delta w, \Psi_m \rangle - \langle p^-, \Psi_m \rangle &= -\langle p^+, \Psi_m \rangle, \\ \langle \partial_t^2 w, \Psi_m \rangle + \frac{1}{\rho_w} \langle \partial_{x_3} p^-, \Psi_m \rangle &= 0.\end{aligned}$$

Using (12), we have

$$\begin{aligned}(-m\omega_m^2 + B\|k_m\|^4) \langle w, \Psi_m \rangle - \langle p^-, \Psi_m \rangle &= -\langle p^+, \Psi_m \rangle, \\ -\omega_m^2 \langle w, \Psi_m \rangle + \frac{1}{\rho_w} \sum_{n \in \mathbb{Z}^3} p_n^- \Theta'_{n_3}(0) \langle \Theta_n, \Psi_m \rangle &= 0,\end{aligned}$$

and furthermore by the identity

$$\begin{aligned}\langle \Theta_n, \Psi_m \rangle &= \left( \frac{T}{2\pi} \int_{-\pi}^{\pi} \exp(int') \exp(-imt') dt' \right) \left( \frac{l_1}{2\pi} \int_{-\pi}^{\pi} \cos(ny_1) \exp(-imy_1) dy_1 \right) \times \\ &\times \left( \frac{l_2}{2\pi} \int_{-\pi}^{\pi} \cos(ny_2) \exp(-imy_2) dy_2 \right) = \begin{cases} Tl_1 l_2, & m = n = 0, \\ \frac{1}{4} Tl_1 l_2, & m = n \neq 0, \\ 0, & m \neq n, \end{cases}\end{aligned}$$

it follows that

$$\begin{aligned}(-m\omega_m^2 + B\|k_m\|^4) \langle w, \Psi_m \rangle - \langle p^-, \Psi_m \rangle &= -\langle p^+, \Psi_m \rangle, \\ -\omega_m^2 \langle w, \Psi_m \rangle + \frac{1}{\rho_w} p_m^- \Theta'_{m_3}(0) Tl_1 l_2 \left\{ 1, \frac{1}{4} \right\} &= 0.\end{aligned}$$

Consequently we have the representation

$$p_m^- = - \left[ (-m\omega_m^2 + B\|k_m\|^4) \frac{\Theta'_{m_3}(0)}{\rho_w \omega_m^2} - \Theta_{m_3}(0) \right]^{-1} \frac{\langle p^+, \Psi_m \rangle}{Tl_1 l_2} \begin{cases} 1, & m = n = 0, \\ 4, & m = n \neq 0. \end{cases}$$

The calculation of  $w_m$  runs analogously.

Thus, applying the definition (19) and  $\alpha_m = \Theta'_{m_3}(0)/\rho_w \omega_m^2 \Theta_{m_3}(0)$ , we can define a transfer function between the hydrodynamic and acoustic fourier coefficients

$$\frac{\langle p^-, \Psi_m \rangle}{\|\Psi_m\|^2} = F(\omega_m, (k_1)_m, (k_2)_m, x_3) \frac{\langle p^+, \Psi_m \rangle}{\|\Psi_m\|^2},\tag{21}$$

where

$$F(\omega_m, (k_1)_m, (k_2)_m, x_3) = - \left[ (-m\omega_m^2 + B\|k_m\|^4) \alpha_m - 1 \right]^{-1} \frac{\Theta_{m_3}(x_3)}{\Theta_{m_3}(0)}.\tag{22}$$

After an inverse Fourier transformation w.r.t.  $k_2$  and an evaluation at  $x_2 = 0$ , Figure 4 shows the different eigenfrequencies.

As a special case we consider the transfer function without backward waves ( $k_3 z + \omega \rho_w = 0$ ). Then it follows that

$$F(\omega_m, (k_1)_m, (k_2)_m, x_3) = - \left[ (-m\omega_m^2 + B\|k_m\|^4) \left( -\frac{ik_3}{\rho_w \omega^2} \right) - 1 \right]^{-1} \exp(-ik_3 x_3),$$

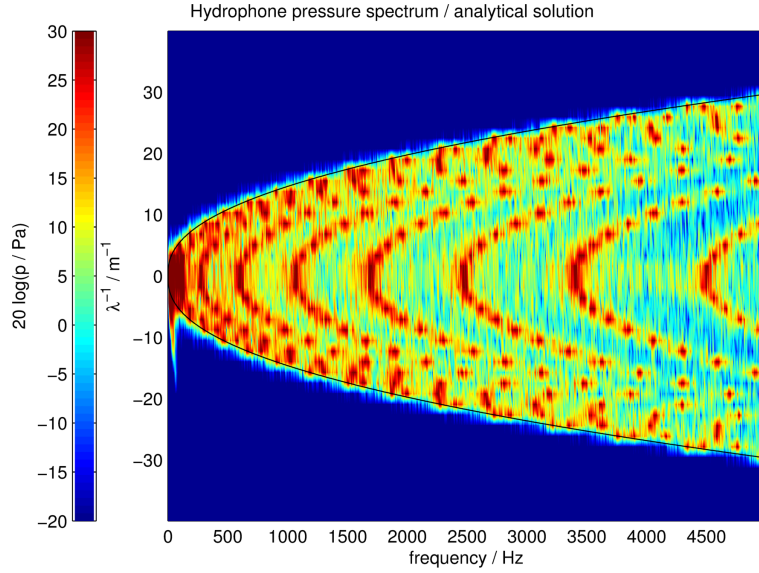


**Figure 4:** Sound Pressure Level (analytical solution): wave-number-frequency plot for towing speed  $u = 4\text{kn}$  and a hydrophone distance of  $0.01\text{m}$ .

which leads for every  $k_2 = \frac{2\pi n_j}{l_j}$  to the dispersion relation

$$-(-m\omega_m^2 + B\|k_m\|^4) - \frac{i\rho_w\omega^2}{k_3} = 0. \quad (23)$$

Notice that the black line from Figures 4-5 represents the dispersion relation for  $k_2 = 0$ .

However, the transfer function is only useful for theoretical observations. In order to compare the analytical solution with the sea trial results, we have to consider damping effects.

### 4.3 Acoustic and bending waves with damping

Inspired by the damped harmonic oscillator we include damping effects in the analytical solution, which are related to the undamped eigenfrequencies of the bending wave equation. In order to do that, we consider the usual harmonic oscillator at position  $x = \hat{x} \exp(-i\omega t)$  with a mass  $m$  and a constant  $k$

$$-m\omega^2 x + kx = 0.$$

Now, the damped harmonic oscillator reads as follows

$$-m\omega^2 x - i2m\eta\omega\omega_0 x + kx = 0,$$

where  $\omega_0 = \sqrt{k/m}$  is the eigenfrequency of the undamped oscillator and  $\eta$  is a normed damping parameter.

Returning to the problem under consideration, the damped transfer function is given by

$$F = - \left[ \left( -m\omega_m^2 + i2m\omega_m\eta\sqrt{\frac{B}{m}}\|k_m\|^2 + B\|k_m\|^4 \right) \alpha_m - 1 \right]^{-1} \frac{\Theta_{m_3}(x_3)}{\Theta_{m_3}(0)}.$$

For the simplicity of notation we have omitted the arguments from the transfer function.

Moreover, in practical configurations it could be useful to provide an anisotropic damping mechanism

$$F = - \left[ \left( -m\omega_m^2 + i2m\omega_m\sqrt{\frac{B}{m}}(\eta_1 k_{m1}^2 + \eta_2 k_{m2}^2) + B\|k_m\|^4 \right) \alpha_m - 1 \right]^{-1} \frac{\Theta_{m_3}(x_3)}{\Theta_{m_3}(0)}. \quad (24)$$



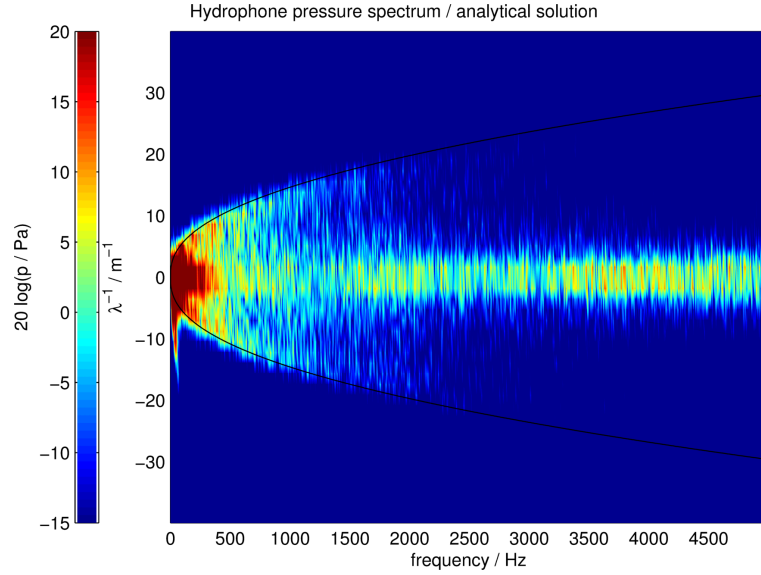


**Figure 5:** Sound Pressure Level (analytical solution with damping  $\eta_1 = 0.3$ ,  $\eta_2 = 2.0$ ): wave-number-frequency plot for towing speed  $u = 4\text{kn}$  and a hydrophone distance of  $0.01\text{m}$ .

## 5 Conclusions

In the present study, it is demonstrated that the problem of flow noise generation and propagation in hull-mounted sonar systems could be solved by an analytical solution. The solution is based on a hydrodynamical source term and considers the fluid structure interaction of bending and acoustic waves w.r.t. different isotropic materials and geometries. Finally, it shows that the accuracy of the analytical solution is within the scope of sea trial measurement accuracies.

## References

- [AK16] Abshagen, J. and Küter, D. and Schäfer, I. and Nejedl, V. Interior Noise from a flow over an obstacle in an underwater towed body. *In preparation*.
- [CH93] Chung, J. and Hulbert, G.M. A Time Integration Algorithm for Structural Dynamics with Improved Numerical Dissipation: The Generalized- $\alpha$  Method. *J. Appl. Mech.*, Vol. 60, 371–375, 1993.
- [JWH00] Jansen, K.E. and Whiting, C.H. and Hulbert, G.M. A Generalized- $\alpha$  Method for Integrating the Filtered Navier-Stokes Equations with a Stabilized Finite Element Method. *Comput. Methods Appl. Mech. Engrg.*, Vol. 190, 305–319, 2000.
- [WH69] Williams, J.E. Ffowcs and Hawkins, D.L. Sound Generation by Turbulence and Surfaces in Arbitrary Motion. *Philosophical Transactions of the Royal Society of London*, Vol. 264, 321–342, 1969.
- [Ho98] Howe, M.S. Acoustics of Fluid-Structure Interactions. *Cambridge Monographs on Mechanics*, 1998.
- [WHea07] Wagner, C. and Hüttl, T. and Sagaut, P. Large-Eddy Simulation for Acoustics. *Cambridge University Press*, 2007.